Journal of Cellular Biochemistry 82:599–609 (2001)

Tissue Specific Metabolism of 1α,25-Dihydroxy-20-epi-Vitamin D_3 Into New Metabolites With Significant Biological Activity: Studies in Rat Osteosarcoma Cells (UMR 106 and ROS 17/2.8)

M-L. Siu-Caldera,[1] D. Sunita Rao,[1] N. Astecker,[1] A. Weiskopf,[2] P. Vouros,[3] K. Konno,[4] T. Fujishima,[4] H. Takayama,[4] S. Peleg,[5] and G. Satyanarayana Reddy[1]*

[1]Department of Pediatrics, Women and Infants' Hospital of Rhode Island, Brown University School of Medicine, Providence, Rhode Island 02905
[2]Cetek Corporation, Marlborough, Massachussetts 01752
[3]Northeastern University, Boston, Massachussetts 02115
[4]Faculty of Pharmaceutical Sciences, Teikyo University, Kanagawa 199-0195, Japan
[5]Department of Medical Specialties, The University of Texas, MD Anderson Cancer Center, Houston, Texas 77030

Abstract In a recent study, we investigated the metabolism of 1α,25-dihydroxy-20-epi-vitamin D_3 (1α,25$(OH)_2$-20-epi-D_3), a potent synthetic vitamin D_3 analog in the isolated perfused rat kidney and proposed that the enhanced biological activity of 1α,25$(OH)_2$-20-epi-D_3 is in part due to its metabolism into stable bioactive intermediary metabolites derived via the C-24 oxidation pathway (Siu-Caldera et al. [1999] J. Steroid. Biochem. Mol. Biol. 71:111–121). It is now well established that 1α,25$(OH)_2D_3$ and its analogs are metabolized in target tissues not only via the C-24 oxidation pathway but also via the C-3 epimerization pathway. As the perfused rat kidney does not express the C-3 epimerization pathway, we could not identify other possible bioactive metabolites of 1α,25$(OH)_2$-20-epi-D_3 such as 1α,25$(OH)_2$-20-epi-3-epi-D_3, derived via the C-3 epimerization pathway. Therefore, we studied the metabolism of 1α,25$(OH)_2$-20-epi-D_3 in rat osteosarcoma cells (UMR 106) which express both the C-24 oxidation and the C-3 epimerization pathways. Our results indicate that 1α,25$(OH)_2$-20-epi-D_3 is metabolized in UMR 106 cells into several metabolites which included not only the previously known metabolites of the C-24 oxidation pathway but also three new metabolites which were labeled as metabolites X, Y1, and Y2. Metabolite X was unequivocally identified as 1α,25$(OH)_2$-20-epi-3-epi-D_3. Eventhough definite structure identification of the metabolites, Y1 and Y2 was not achieved in our present study, we determined that the metabolite Y1 is produced from 1α,25$(OH)_2$-20-epi-D_3 and the metabolite Y2 is produced from 1α,25$(OH)_2$-20-epi-3-epi-D_3. We also noted the production of both 1α,25$(OH)_2$-20-epi-3-epi-D_3 and the two metabolites Y1 and Y2 in different rat osteosarcoma cells (ROS 17/2.8) which express only the C-3 epimerization pathway but not the C-24 oxidation pathway. Furthermore, we investigated the metabolism of 1α,25$(OH)_2$-20-epi-D_3 in the isolated perfused rat kidney in an earlier study. The results of this study indicated that the rat kidney unlike rat osteosarcoma cells did not produce either 1α,25$(OH)_2$-20-epi-3-epi-D_3 or the metabolites Y1 and Y2. Thus, it appears that the metabolites Y1 and Y2, like 1α,25$(OH)_2$-20-epi-3-epi-D_3, are produced only in specific tissues. Preliminary biological activity of each new metabolite is assessed by measuring its ability to generate VDR-mediated gene transcription. 1α,25$(OH)_2$-20-epi-3-epi-D_3 was found to be almost equipotent to 1α,25$(OH)_2$-20-epi-D_3 while the metabolites, Y1 and Y2 were found to be less active. The metabolite Y1 when compared to the metabolite Y2

Abbreviations used: 1α,25$(OH)_2D_3$, 1α,25-dihydroxyvitamin D_3; 1α,25$(OH)_2$-3-epi-D_3, 1α,25-dihydroxy-3-epi-vitamin D_3; 1α,24(R),25$(OH)_3D_3$, 1α,24(R),25-trihydroxyvitamin D_3; 1α,25$(OH)_2$-24-oxo-D_3, 1α,25-dihydroxy-24-oxovitamin D_3; 1α,23(S),25$(OH)_3$-24-oxo-D_3, 1α,23(S),25-trihydroxy-24-oxovitamin D_3; 1α,23$(OH)_2$-24,25,26,27-tetranor D_3 or C-23 alcohol, 1α,23-dihydroxy-24,25,26,27-tetranorvitamin D_3; 1α,25$(OH)_2$-20-epi-D_3, 1α,25-dihydroxy-20-epi-vitamin D_3; 1α,25$(OH)_2$-20-epi-3-epi-D_3, 1α,25-dihydroxy-20-epi-3-epi-vitamin D_3; 1α,24(R)25$(OH)_3$-20-epi-D_3, 1α,24(R),25-trihydroxy-20-epi-vitamin D_3; 1α,25$(OH)_2$-20-epi-24-oxo-D_3, 1α,25-dihydroxy-20-epi-24-oxo-vitamin D_3.

Grant sponsor: NIH to GSR; Grant number: DK52488; Grant sponsor: NIH to SP; Grant number: DK50583.

*Correspondence to: Dr. G. Satyanarayana Reddy, Department of Pediatrics, Women and Infants' Hospital, 101 Dudley Street, Providence, Rhode Island 02905.
E-mail: sreddy@wihri.org

Received 3 January 2001; Accepted 11 April 2001

has higher biological activity and its potency is almost equal to 1α,25(OH)$_2$D$_3$. In summary, we report for the first time tissue specific metabolism of 1α,25(OH)$_2$-20-epi-D$_3$ into several bioactive metabolites which are derived not only via the previously established C-24 oxidation and C-3 epimerization pathways but also via a new pathway. J. Cell. Biochem. 82: 599–609, 2001.

Key words: 1α,25(OH)$_2$-20-epi-D$_3$; C-24 oxidation pathway; C-3 epimerization pathway; new pathway; tissue specific metabolism; UMR 106 cells; ROS 17/2.8 cells

Recently numerous analogs of the secosteroid hormone, 1α,25-dihydroxyvitamin D$_3$ (1α,25(OH)$_2$D$_3$) with several different side chain modifications have been synthesized [Bouillon et al., 1995]. One class of analogs with 20-epi modification, have become prominent because of their unique biological properties. These 20-epi vitamin D analogs in which the methyl group at C-20 is in the unnatural orientation have been shown to decrease cell proliferation and promote cell differentiation with a potency several orders of magnitude greater than that of 1α,25(OH)$_2$D$_3$ [Binderup et al., 1991; Elstner et al., 1994,1996; Gniadecki, 1997]. One of the several proposed mechanisms for the enhanced biological activities of 20-epi vitamin D analogs when compared to 1α,25(OH)$_2$D$_3$ is the differences in their target tissue metabolism [Dilworth et al., 1994; Siu-Caldera et al., 1999a].

1α,25(OH)$_2$D$_3$ is metabolized in its target tissues via modifications of both the side chain and the A-ring. The C-24 oxidation pathway is initiated by hydroxylation at C-24. This pathway is the main side chain modification pathway and leads to the formation of the end product, calcitroic acid [Makin et al., 1989; Reddy and Tserng, 1989; Bouillon et al., 1995; Brown et al., 1999a]. The C-23 and C-26 oxidation pathways are initiated by hydroxylations at C-23 and C-26, respectively. These minor side chain modification pathways together lead to the formation of the end product, 1α,25(OH)$_2$D$_3$-lactone [Ishizuka and Norman, 1987; Bouillon et al., 1995]. The C-3 epimerization pathway is initiated by epimerization of the hydroxyl group at C-3. This newly discovered A-ring modification pathway leads to the conversion of 1α,25(OH)$_2$D$_3$ into 1α,25-dihydroxy-3-epi-vitamin D$_3$ (1α,25(OH)$_2$-3-epi-D$_3$) [Reddy et al., 1994, 1997, 2001].

In a recent study, we studied the metabolism of 1α,25-dihydroxy-20-epi-vitamin D$_3$ (1α,25(OH)$_2$-20-epi-D$_3$) (Fig. 1), the simplest of the 20-epi vitamin D analogs in the isolated perfused rat kidney. The results of this study indicated that 1α,25(OH)$_2$-20-epi-D$_3$ is metabolized in the rat kidney into two stable, bioactive intermediary metabolites (1α,24(R),25(OH)$_3$-20-epi-D$_3$ and 1α,25(OH)$_2$-24-oxo-20-epi-D$_3$) derived via the C-24 oxidation pathway. Thus, we have put forward the concept that the enhanced biological activity of 1α,25(OH)$_2$-20-epi-D$_3$ is in part due to its metabolism into stable bioactive intermediary metabolites derived via the C-24 oxidation pathway [Siu-Caldera et al., 1999a]. However, in the same study, we could not identify other possible bioactive intermediary metabolites such as 1α,25(OH)$_2$-20-epi-3-epi-D$_3$ derived via the C-3 epimerization pathway as the rat kidney does not express the C-3 epimerization pathway. Therefore, in the present study, we investigated the metabolism of 1α,25(OH)$_2$-20-epi-D$_3$ in two different rat osteosarcoma cells (UMR 106 and ROS 17/2.8) which are known to express the C-3 epimerization pathway [Siu-Caldera et al., 1999b]. Our results indicated that 1α,25(OH)$_2$-20-epi-D$_3$ is metabolized in rat osteosarcoma cells into several intermediary metabolites which include not only the previously known metabolites of the C-24 oxidation pathway but also three new metabolites. In this paper, we report the isolation and identification and the tissue specific production of these new metabolites along with the preliminary evaluation of their biological activity.

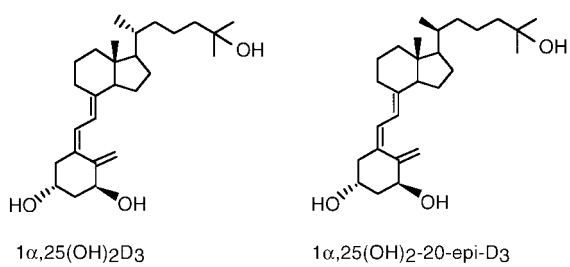

Fig. 1. Chemical structures of 1α,25(OH)$_2$D$_3$ and 1α,25(OH)$_2$-20-epi-D$_3$.

MATERIALS AND METHODS

Materials

UMR 106 cells were purchased from ATCC (Rockville, MD). ROS 17/2.8 cells were obtained from M.D. Anderson Cancer Center, Houston, TX. Streptomycin, penicillin, McCoy's, Dulbecco's modified Eagle's media (DMEM), and Ham's F-12 media were obtained from Life Technologies (Gaithersburg, MD). Fetal calf serum (FCS) was purchased from Hyclone (Logan, UT). Tissue culture flasks and high performance liquid chromatography (HPLC) reagents were purchased from Baxter (McGaw Park, IL).

Vitamin D Compounds

1α,25(OH)$_2$D$_3$ and 1α,25(OH)$_2$-3-epi-D$_3$ were synthesized at Hoffmann-La Roche, Nutley, NJ. 1α,25(OH)$_2$-20-epi-D$_3$ and 1α,25-dihydroxy-20-epi-3-epi-vitamin D$_3$ (1α,25(OH)$_2$-20-epi-3-epi-D$_3$) were synthesized at Teikyo University, Kanagawa, Japan. All of the natural metabolites of both 1α,25(OH)$_2$D$_3$ and 1α,25(OH)$_2$-20-epi-D$_3$ derived via the C-24 oxidation pathway were produced using the kidney perfusion system as previously described [Reddy et al., 1982, 1987]. All the vitamin D$_3$ compounds were quantitated by UV spectroscopic analysis assuming an extinction coefficient (λ_{265} nm) of 18300 dm^3/mol/cm.

High Performance Liquid Chromatography and Gas Chromatography/Mass Spectrometry (GC/MS) Analysis

HPLC analysis of the lipid extracts from the cells and media was performed with a Waters System Controller (model 600E) equipped with a photodiode array detector (model PDA 990) to monitor ultraviolet (UV) absorbing material at 265 nm (Waters Associates, Milford, MA). The vitamin D compounds were isolated and purified using both straight and reverse phase HPLC systems. Analysis by straight phase HPLC involved the use of a Zorbax-SIL column (9 × 250 mm) (Dupont, Wilmington, DE) eluted with three different solvent mixtures at a flow rate of 2 mL/min. The solvent mixtures used were as follows: 10% isopropanol:hexane (HPLC system-I); 2% isopropanol:hexane (HPLC system-II); and 4% isopropanol:methylene chloride (HPLC system-III). Analysis by reverse phase HPLC involved the use of a Zorbax-ODS column (4.5 × 250 mm) (Dupont, Wilmington, DE) eluted with 25% water in methanol at a flow rate of 1 mL/min (HPLC system-IV).

GC/MS analysis was performed using a Hewlett-Packard GC-MSD system which is equipped with a 5890 series II chromatograph, a 5971 mass selective detector and a 7673 GC autosampler (Hewlett-Packard, Wilmington, DE). The vitamin D compounds were trimethylsilylated in 30 μL of a 1:1 mixture of acetonitrile and Power SIL-Prep (Alltech Associates, Inc., Deerfield, IL) and incubated at 70°C for 15 min. The trimethylsilyl ether derivatives were analyzed in duplicate. Samples were analyzed on an HP-5 capillary column (30 m × 0.25 mm × 0.25 μm) using a temperature program ranging from 140 to 320°C with a 20°C/min temperature gradient. Full scan electron impact spectra ($m/z = 50-650$) were acquired for each experiment.

Cells and Cell Culture

UMR 106 cells were maintained in McCoy's culture media supplemented with 10% FCS and antibiotics (penicillin (100 IU/mL) and streptomycin (100 μg/mL)). ROS 17/2.8 cells were maintained in DMEM and Ham's F-12 media (50:50; v/v) supplemented with 10% FCS and antibiotics (penicillin (100 IU/mL) and streptomycin (100 μg/mL)). Cell culture medium was changed every 3–4 days. The cells were subcultured when ~80% confluent and were not subcultured beyond five passages. For the metabolism studies, 3×10^6 cells were seeded in T150 tissue culture bottles and were grown to confluence. The incubations were carried out at 37°C in a humidified atmosphere under 5% CO_2.

Metabolism of 1α,25(OH)$_2$D$_3$ and 1α,25(OH)$_2$-20-epi-D$_3$ in UMR 106 and ROS 17/2.8 Cells

Confluent UMR 106 or ROS 17/2.8 cells were incubated with 1 μM concentration of either 1α,25(OH)$_2$D$_3$ or 1α,25(OH)$_2$-20-epi-D$_3$ in 50 mL media containing 10% FCS. The incubations were stopped at 24 h with 10 mL of methanol. The lipids from both cells and media were extracted for HPLC analysis, using the extraction procedure described earlier [Reddy and Tserng, 1989]. Control incubations without cells containing only media and the vitamin D compounds were also performed.

Transcription Assay

The vitamin D receptor (VDR)-mediated transcriptional activity of each of the new

vitamin D compound is tested using the following assay. ROS 17/2.8 cells were plated in 35 mm dishes at a density of 3×10^5/dish in Dulbecco's modified eagle's medium (DMEM) (Life Technologies, Grand Island, NY) and 10% FCS (Hyclone, Logan, UT). Forty-eight hours later, the cells were transfected with plasmid (2 μg/dish) containing the vitamin D response element (VDRE) from the human osteocalcin gene (GGTGACTCACCGGGTGAACGGGGGCATT) [Ozono et al., 1990]. This response element was inserted upstream of the thymidine kinase promoter/growth hormone fusion gene. All transfections were performed by the DEAE dextran method [Lopata et al., 1984]. The cells were treated for 1 min with 10% dimethyl sulfoxide, washed three times with phosphate buffered saline and DMEM was added containing 10% FCS and the vitamin D compounds at the indicated concentrations. Forty eight hours later, medium samples were collected and growth hormone production from the reporter gene was measured by radioimmunoassay as described by the manufacturer (Nichols Institute, San Juan Capistrano, CA).

Statistics

Values were calculated as mean±standard deviation (SD). Significance levels were determined by Student's *t*-test.

RESULTS

Comparison of the Metabolism of 1α,25(OH)$_2$D$_3$ With That of 1α,25(OH)$_2$-20-epi-D$_3$ in UMR 106 Cells

The HPLC profiles and UV spectra of 1α,25(OH)$_2$D$_3$ (Panel A1) and 1α,25(OH)$_2$-20-epi-D$_3$ (Panel B1) and their respective metabolites produced by UMR 106 cells during a 24 h incubation period are shown in Figure 2. 1α,25(OH)$_2$D$_3$ was metabolized into several polar metabolites namely, 1α,25-dihydroxy-24-oxovitamin D$_3$ (1α,25(OH)$_2$-24-oxo-D$_3$), 1α,23-dihydroxy-24,25,26,27-tetranorvitamin D$_3$ (1α,23(OH)$_2$-24,25,26,27-tetranor-D$_3$ or C-23 alcohol), 1α,23(S),25-trihydroxy-24-oxovitamin D$_3$ (1α,23(S),25(OH)$_3$-24-oxo-D$_3$) and 1α,24(R),25-trihydroxyvitamin D$_3$ (1α,24(R),25(OH)$_3$D$_3$) derived via the C-24 oxidation pathway and the less polar metabolite namely, 1α,25(OH)$_2$-3-epi-D$_3$ derived via the C-3 epimerization pathway (Fig. 2, panel A1). These results are similar to those reported previously [Siu-Caldera et al., 1999b]. Unlike 1α,25(OH)$_2$D$_3$, most of 1α,25(OH)$_2$-20-epi-D$_3$, was metabolized by the UMR 106 cells (Fig. 2, Panel B1, peak 1) into several metabolites which included two polar metabolites (peaks 2 and 3) and three less polar metabolites (peaks X, Y1, and Y2). Metabolite 3 was identified as 1α,24(R),25-trihydroxy-20-epi-vitamin D$_3$ (1α,24(R),25(OH)$_3$-20-epi-D$_3$) and metabolite 2 was identified as 1α,25-dihydroxy-20-epi-24-oxovitamin D$_3$ (1α,25(OH)$_2$-20-epi-24-oxo-D$_3$). The identity of each metabolite was established through its coelution with synthetic standard using both straight and reverse phase HPLC systems and GC/MS (data not shown). Like in the perfused rat kidney [Siu-Caldera et al., 1999a], the further metabolites of 1α,25(OH)$_2$-24-oxo-20-epi-D$_3$ namely, 1α,23,25(OH)$_3$-24-oxo-20-epi-D$_3$ and C-23 alcohol were also not detected in UMR 106 cells indicating partial metabolic block in the C-24 oxidation pathway. This partial metabolic block leads to the accumulation of 1α,25(OH)$_2$-24-oxo-20-epi-D$_3$ and its precursor, 1α,24(R),25(OH)$_3$-20-epi-D$_3$ in UMR 106 cells. The less polar metabolites X, Y1, and Y2 exhibited UV spectra which are typical to vitamin D compounds (Fig. 2, panel B1, inset). The details of the process of identification of these metabolites are described in the sections below. The control incubation studies indicated that both 1α,25(OH)$_2$D$_3$ (Fig. 2, Panel A2) and 1α,25(OH)$_2$-20-epi-D$_3$ (Fig. 2, Panel B2) did not undergo any chemical change or breakdown either during the incubation period or during the extraction procedure.

Metabolite X: Identification as 1α,25(OH)$_2$-20-epi-3-epi-D$_3$ by GC/MS and HPLC

Metabolite X was purified using HPLC systems-II, III, and IV described in the Materials and Methods section. Figure 3 shows the mass spectrum of the trimethylsilylated metabolite X (upper panel) which is identical to the trimethylsilylated 1α,25(OH)$_2$-20-epi-3-epi-D$_3$ synthetic standard (lower panel). Both spectra exhibited a molecular ion at m/z 632 and the characteristic fragments at m/z 542 and 452 due to losses of one and two trimethylsilylated hydroxyl groups, respectively. The loss of 131 Da from the A-ring (m/z 501) and the detection of ion fragment at m/z 217, arising from A-ring cleavage, indicate the presence of hydroxyl groups at C-1 and C-3 on the A-ring. The mass at m/z 131 represents cleavage across the C-24/C-25 bond on the side chain. In addition to

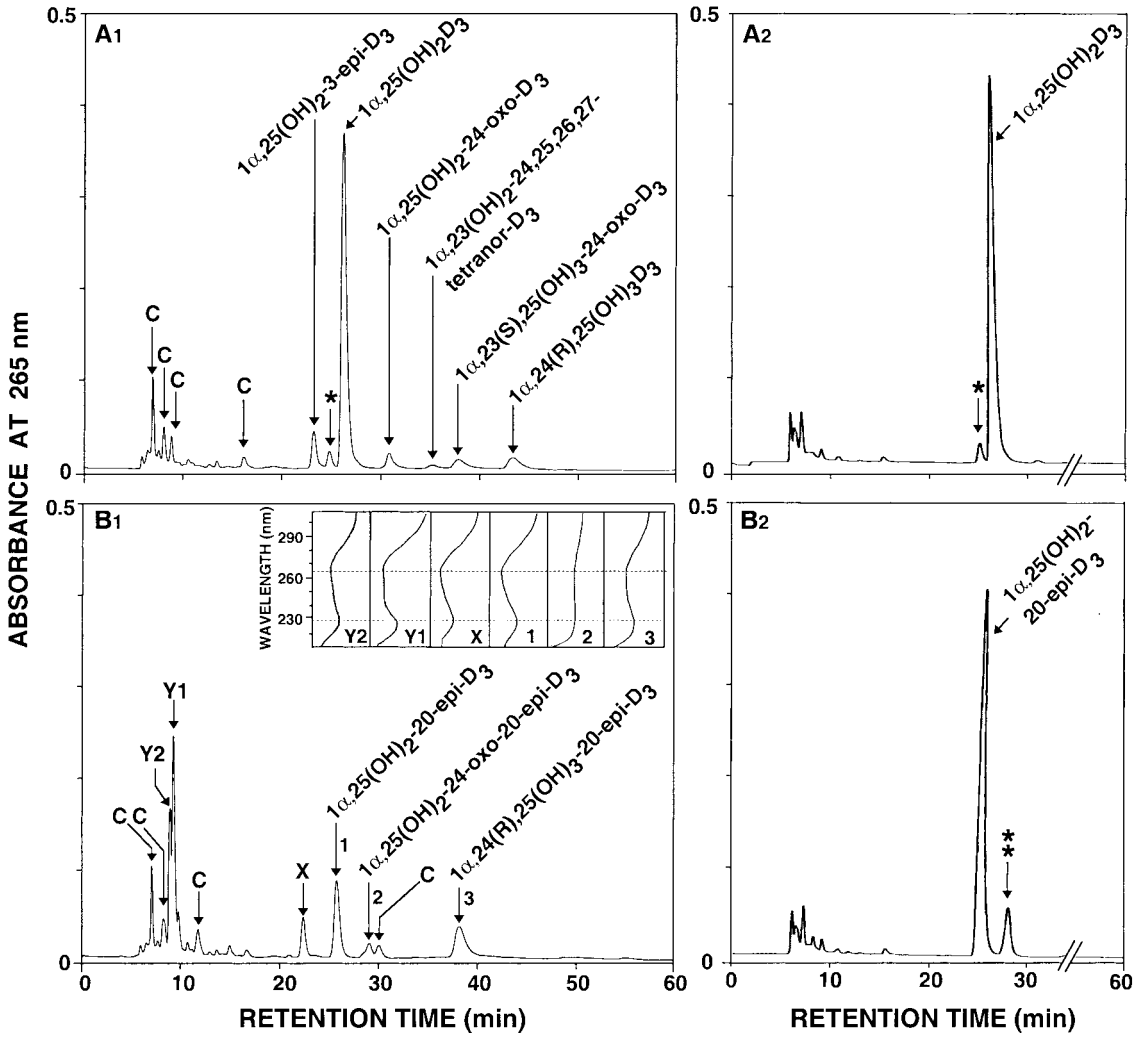

Fig. 2. HPLC profiles of the lipid extracts of various vitamin D metabolites produced in UMR 106 cells incubated with either 1α,25(OH)$_2$-20-epi-D$_3$ (Panels B1 and B2) or 1α,25(OH)$_2$D$_3$ (Panels A1 and A2). HPLC was performed using a Zorbax-SIL column (9 × 250 mm) eluted with hexane-isopropanol (90:10) at a flow rate of 2 mL/min. The various metabolites of 1α,25(OH)$_2$-20-epi-D$_3$ and 1α,25(OH)$_2$D$_3$ were monitored by their UV absorbance at 265 nm. Panels A1 and B1: HPLC profiles of 1α,25(OH)$_2$D$_3$ (A1) or 1α,25(OH)$_2$-20-epi-D$_3$ (B1) and their various metabolites. UV spectra of the substrate and the metabolite peaks are shown in the inset. Panels A2 and B2: HPLC profiles of control incubations (with no cells) using 1α,25(OH)$_2$D$_3$ (A2) or 1α,25(OH)$_2$-20-epi-D$_3$ (B2) as substrate. The single asterisk (panels A1 and A2) represents pre-1α,25(OH)$_2$D$_3$ and the double asterisk (panel B2) represents pre-1α,25(OH)$_2$-20-epi-D$_3$. Peaks X,Y1, and Y2 (panel B1) are the three new metabolites. All the peaks represented by 'C' are the lipid contaminants.

the identical mass spectra, the retention times (rt) on GC/MS also confirmed the identity of the metabolite X as 1α,25(OH)$_2$-20-epi-3-epi-D$_3$. The retention time of metabolite X (rt 16.24 min) was similar to that of the synthetic standard (rt 16.25 min). The final proof for unequivocal identification of metabolite X was obtained by HPLC. The retention time of the metabolite X is compared to that of each of the four diastereomers of 1α,25(OH)$_2$-20-epi-D$_3$. Metabolite X comigrated only with the synthetic standard of 1α,25(OH)$_2$-20-epi-3-epi-D$_3$ on both straight and reverse phase HPLC systems (Table I).

Metabolites Y1 and Y2: Identification of Their Parent Substrates

The metabolites Y1 and Y2 were purified using the HPLC systems-II and III described in the Materials and Methods section. Each individual metabolite was then subjected to GC/MS. The GC/MS analysis of both metabolites Y1

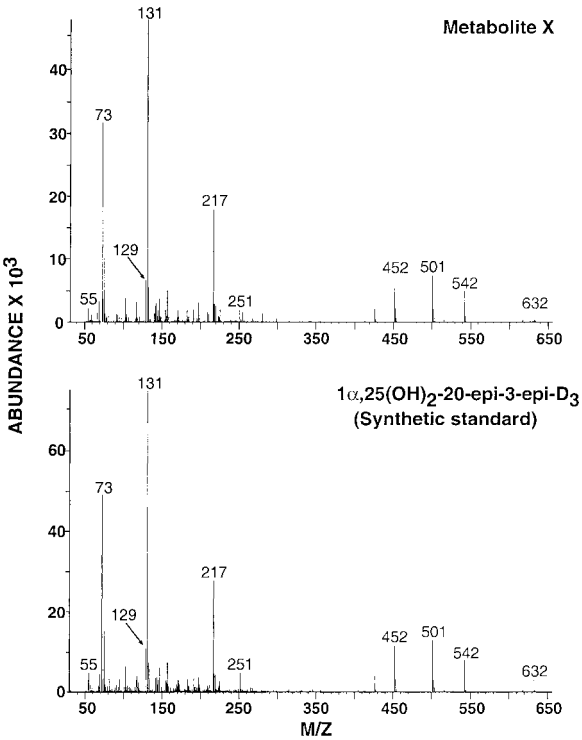

Fig. 3. Mass spectra of trimethylsilylate derivatives of the synthetic standard of 1α,25(OH)$_2$-20-epi-3-epi-D$_3$ and of metabolite X produced in UMR 106 cells. Upper panel: Metabolite X, retention time 16.24 min; Lower panel: Synthetic standard of 1α,25(OH)$_2$-20-epi-3-epi-D$_3$, retention time 16.25 min.

and Y2 indicated that these metabolites were complex A-ring modified metabolites with an intact 25-hydroxylated side chain (data not shown). It was realized that ^{1}H-NMR studies were needed for definite identification of these metabolites. As only limited amounts of these metabolites were available to us, we could not perform ^{1}H-NMR studies. However, we were able to identify the parent substrates of the metabolites Y1 and Y2 by performing the following experiment.

Confluent UMR 106 cells were incubated with either 1α,25(OH)$_2$-20-epi-D$_3$ or 1α,25(OH)$_2$-20-epi-3-epi-D$_3$ at 1 μM substrate concentration for 8 h. Figure 4 shows the HPLC profiles and UV spectra of 1α,25(OH)$_2$-20-epi-D$_3$ (panel A) and 1α,25(OH)$_2$-20-epi-3-epi-D$_3$ (panel B) and their respective metabolites produced by UMR 106 cells during an 8 h incubation period. The present 8 h incubation study like our prior 24 h incubation study also indicates that 1α,25(OH)$_2$-20-epi-D$_3$ is metabolized into 1α,24(R),25(OH)$_3$-20-epi-D$_3$, 1α,25(OH)$_2$-24-oxo-20-epi-D$_3$, and 1α,25(OH)$_2$-20-epi-3-epi-D$_3$ derived via both C-24 oxidation and C-3 epimerization pathways and into metabolites Y1 and Y2 derived via the new pathway. On the contrary, UMR 106 cells incubated with 1α,25(OH)$_2$-20-epi-3-epi-D$_3$ produced only metabolite Y2 in significant amounts. This finding indicates that 1α,25(OH)$_2$-20-epi-3-epi-D$_3$ is the parent substrate for the metabolite Y2. Thus, we were able to conclude that metabolite Y1 is produced from the parent, 1α,25(OH)$_2$-20-epi-D$_3$, and the metabolite Y2 is produced from 1α,25(OH)$_2$-20-epi-3-epi-D$_3$. The results of these studies for the first time provided evidence to indicate that 1α,25(OH)$_2$-20-epi-D$_3$ is metabolized in UMR 106 cells through three different pathways as shown in Figure 5.

Relative Amounts of Unmetabolized Substrate and the Metabolites of 1α,25(OH)$_2$D$_3$ and 1α,25(OH)$_2$-20-epi-D$_3$ Produced by UMR 106 Cells

Metabolism studies were performed in triplicate in order to calculate the relative amounts of unmetabolized substrate and the metabolites of 1α,25(OH)$_2$D$_3$ and 1α,25(OH)$_2$-20-epi-D$_3$. The UMR 106 cells were incubated with either 1α,25(OH)$_2$D$_3$ or 1α,25(OH)$_2$-20-epi-D$_3$ at 1 μM concentration for 24 h. The results are shown in Figure 6. It can be seen that the

TABLE I. Retention Times of 1α,25(OH)$_2$-20-epi-D$_3$, its Three Diastereomers and Metabolite X

Vitamin D compounds	A-ring Hydroxyl group orientation	Retention time (min)	
		Straight phase HPLC	Reverse phase HPLC
1α,25(OH)$_2$-20-epi-D$_3$	1α,3β	24.96	24.44
1α,25(OH)$_2$-20-epi-3-epi-D$_3$	1α,3α	21.93	23.19
1β,25(OH)$_2$-20-epi-D$_3$	1β,3β	25.10	24.40
1β,25(OH)$_2$-20-epi-3-epi-D$_3$	1β,3α	23.08	26.49
Metabolite X		21.91	23.08

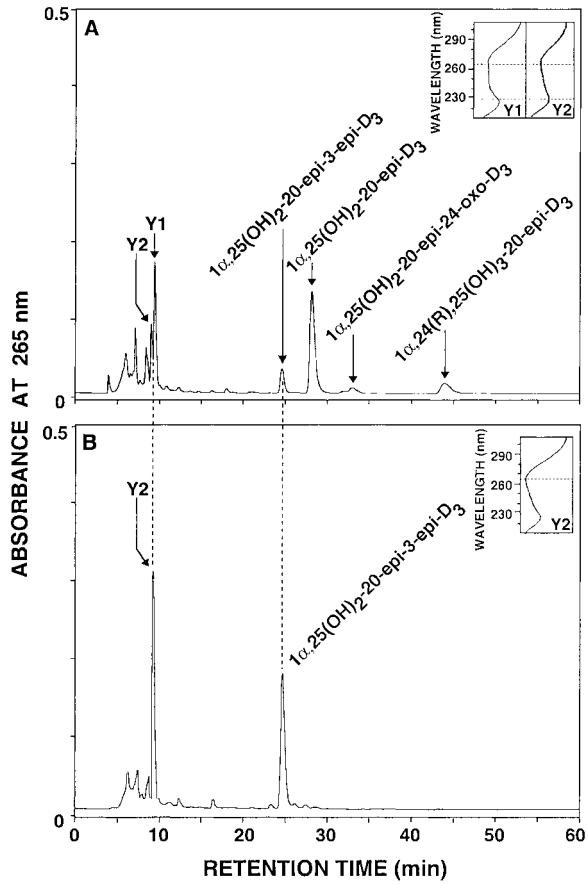

Fig. 4. HPLC profiles and UV spectra of various vitamin D metabolites produced in UMR 106 cells incubated with 1 μM concentration of either 1α,25(OH)$_2$-20-epi-D$_3$ (Panel A) or 1α,25(OH)$_2$-20-epi-3-epi-D$_3$ (Panel B) for 8 h. HPLC analysis was performed under the same chromatographic conditions as described in the legend for Figure 2.

amount of unmetabolized 1α,25(OH)$_2$D$_3$ (Fig. 6, panel A) was about six times greater than that of the unmetabolized 1α,25(OH)$_2$-20-epi-D$_3$ ($P < 0.001$) indicating greater metabolic stability for 1α,25(OH)$_2$D$_3$. There was no significant difference between the amounts of the metabolites of 1α,25(OH)$_2$D$_3$ and 1α,25(OH)$_2$-20-epi-D$_3$ derived via either the C-24 oxidation pathway or the C-3 epimerization pathway (Fig. 6, panel B). However, due to the selective metabolism of 1α,25(OH)$_2$-20-epi-D$_3$ into less polar metabolites Y1 and Y2 (LPMs) a significant difference is noted between the amounts of the total metabolites of 1α,25(OH)$_2$D$_3$ and 1α, 25(OH)$_2$-20-epi-D$_3$. The amount of LPMs produced from 1α, 25(OH)$_2$-20-epi-D$_3$ (Fig. 6, panel B) was about four times greater than the amount of remaining unmetabolized substrate, and about eight times greater than either the C-3 epimer or the amount of the total metabolites derived via the C-24 oxidation pathway ($P < 0.001$). Furthermore, the formation of LPMs was not detected when 1α,25(OH)$_2$D$_3$ was used as the substrate indicating that 1α,25(OH)$_2$-20-epi-D$_3$ is the preferred substrate for the enzyme(s) responsible for the production of the LPMs.

Tissue Specific Metabolism of 1α,25(OH)$_2$-20-epi-D$_3$

The metabolism of 1α,25(OH)$_2$-20-epi-D$_3$ was examined in ROS 17/2.8 cells to determine the existence of the new pathway in tissues in which the C-24 oxidation pathway is not expressed. It has been shown before that ROS 17/2.8 cells do not express the C-24 oxidation pathway but express the C-3 epimerization pathway [Siu-Caldera et al., 1999b]. Figure 7 shows the HPLC profile of 1α,25(OH)$_2$-20-epi-D$_3$ and its metabolites produced by ROS 17/2.8 cells during a 8 h incubation period. As reported previously, ROS 17/2.8 cells produced none of the metabolites of the C-24 oxidation pathway. However, these cells like the UMR 106 cells, were able to metabolize 1α,25(OH)$_2$-20-epi-D$_3$ into 1α,25(OH)$_2$-20-epi-3-epi-D$_3$ and the two metabolites (Y1 and Y2). The identity of all the three metabolites

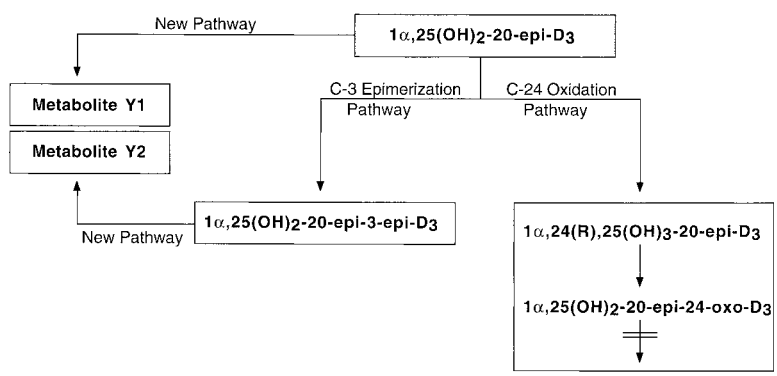

Fig. 5. Pathways of 1α,25(OH)$_2$-20-epi-D$_3$ metabolism in UMR 106 cells.

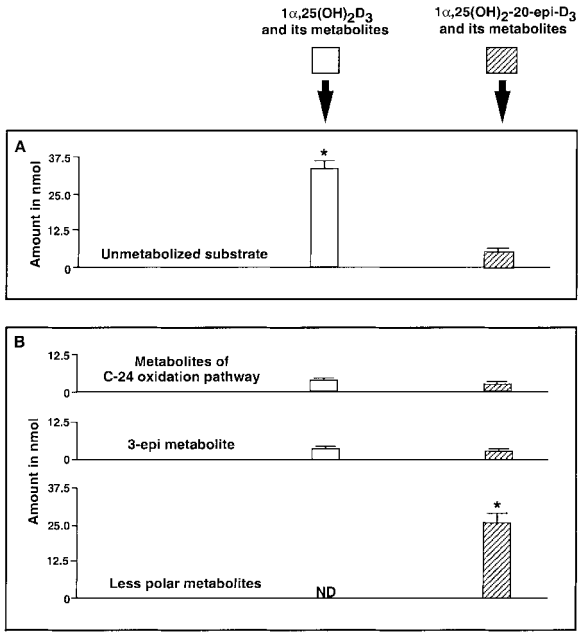

Fig. 6. Relative amounts of unmetabolized substrate and the various metabolites of $1\alpha,25(OH)_2$-20-epi-D_3 (hatched bars) and $1\alpha,25(OH)_2D_3$ (open bars) produced in UMR 106 cells incubated with 1 μM concentration of each compound for 24 h. **Panel A:** Unmetabolized substrates of $1\alpha,25(OH)_2D_3$ and $1\alpha,25(OH)_2$-20-epi-D_3. **Panel B:** Various metabolites of $1\alpha,25(OH)_2$-20-epi-D_3 and $1\alpha,25(OH)_2D_3$. Each value represents the mean±SD (n = 3) (*$P < 0.001$).

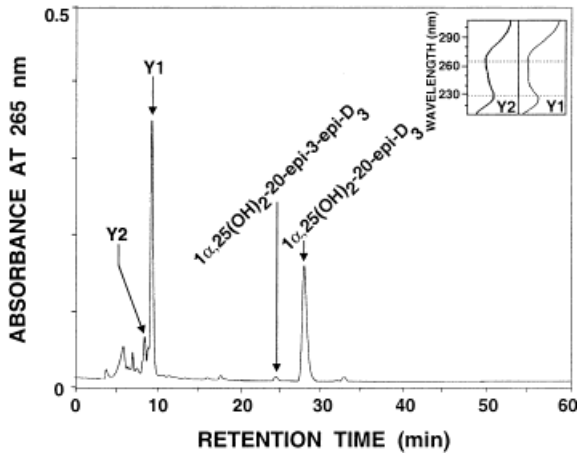

Fig. 7. HPLC profiles and UV spectra of various vitamin D metabolites produced in ROS 17/2.8 cells incubated with 1 μM concentration of $1\alpha,25(OH)_2$-20-epi-D_3 for 8 h. HPLC analysis was performed under the same chromatographic conditions as described in the legend for Figure 2.

produced by ROS 17/2.8 cells was established as described earlier.

The results of our present study together with the results of our previous study investigating the metabolism of $1\alpha,25(OH)_2$-20-epi-D_3 in the perfused rat kidney [Siu-Caldera et al., 1999a] can be summarized as follows: UMR 106 cells metabolize $1\alpha,25(OH)_2$-20-epi-D_3 via all the three pathways (C-24 oxidation, C-3 epimerization, and the new pathways). ROS 17/2.8 cells, which do not express the C-24 oxidation pathway metabolize $1\alpha,25(OH)_2$-20-epi-D_3 via both the C-3 epimerization pathway and the new pathway. The perfused rat kidney, which does not express the C-3 epimerization pathway, metabolizes $1\alpha,25(OH)_2$-20-epi-D_3 only via the C-24 oxidation pathway. Thus, these results when put together led us to develop the concept that the metabolism of $1\alpha,25(OH)_2$-20-epi-D_3 is tissue specific.

Transcriptional Activity

The biological activity of each new metabolite ($1\alpha,25(OH)_2$-3-epi-D_3, metabolites Y1 and Y2), was assessed by its ability to induce VDR-mediated transcription using ROS 17/2.8 cells which had been transfected with a growth hormone reporter gene containing a VDRE from the human osteocalcin gene (ocVDRE/GH). At maximum concentration (1×10^{-7} M), $1\alpha,25(OH)_2$-3-epi-D_3 expressed 25% of the transcriptional activity exerted by $1\alpha,25(OH)_2D_3$ (Fig. 8). Unlike the $1\alpha,25(OH)_2$-3-epi-D_3, $1\alpha,25(OH)_2$-20-epi-3-epi-D_3 and the metabolite Y1 exerted similar transcriptional activity as their parent, $1\alpha,25(OH)_2$-20-epi-D_3, while the metabolite Y2

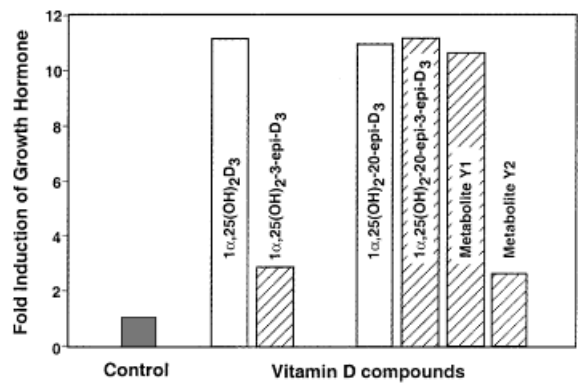

Fig. 8. Transcriptional activity of vitamin D compounds. ROS 17/2.8 cells were transfected by the DEAE-dextran method with a thymidine kinase-growth hormone (TK/GH) fusion gene containing the osteocalcin VDRE (ocVDRE). Immediately after transfection, medium containing 10% FCS and the respective vitamin D compounds (1×10^{-7}M) were added to the cultures. Forty-eight hours later, medium samples were collected and growth hormone levels were determined by radioimmunoassay. Each value is the average of duplicate transfections.

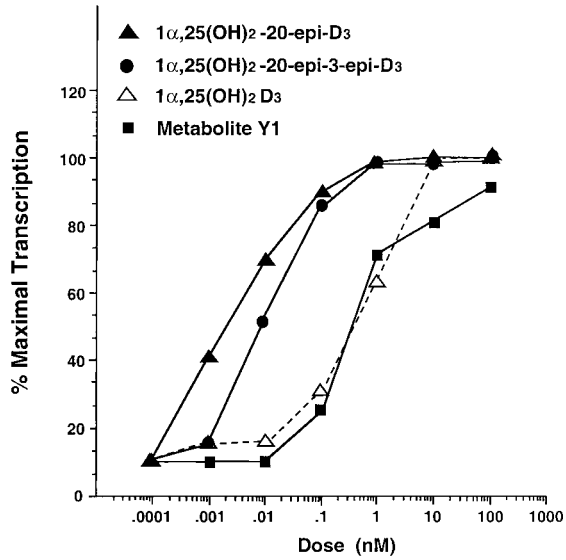

Fig. 9. Dose-response of transcriptional activity of vitamin D compounds in ROS 17/2.8 cells. Dose-response effect on transcription of the vitamin D compounds was determined in ROS 17/2.8 cells as described in the legend for Figure 8. Each point of the dose-response curve is the average of duplicate transfections.

expressed only 25% of the activity exerted by the parent compound (Fig. 8).

Since 1α,25(OH)$_2$D$_3$, 1α,25(OH)$_2$-20-epi-D$_3$, 1α,25(OH)$_2$-20-epi-3-epi-D$_3$ and metabolite Y1 exhibited significant transcriptional activities at maximum concentration, we next examined the transcriptional activities of these metabolites in a dose-response study. Figure 9 shows that the VDR-mediated transcriptional activity was dose-dependent for all the metabolites tested and the ED$_{50}$ for transcriptional activity of 1α,25(OH)$_2$D$_3$, 1α,25(OH)$_2$-20-epi-D$_3$, 1α,25(OH)$_2$-20-epi-3-epi-D$_3$, and metabolite Y1 were 5×10^{-10} M, 2×10^{-12} M, 9×10^{-12} M and 3×10^{-10} M, respectively. Thus, 1α,25(OH)$_2$-20-epi-3-epi-D$_3$ was almost as active as its parent, 1α,25(OH)$_2$-20-epi-D$_3$ in its ability to induce VDR-mediated transcription and both of these compounds are about 100-fold more potent than 1α,25(OH)$_2$D$_3$. Also, although the metabolite Y1 was not as active as its parent, 1α,25(OH)$_2$-20-epi-D$_3$ in its ability to induce VDR-mediated transcription, the metabolite still retained significant biological activity and it was almost equipotent to 1α,25(OH)$_2$D$_3$.

DISCUSSION

In our present study, we report the metabolism of 1α,25(OH)$_2$-20-epi-D$_3$ into several bioactive intermediary metabolites in rat osteosarcoma cells. These metabolites are derived not only via the previously established C-24 oxidation and C-3 epimerization pathways, but also via a new pathway (Fig. 5). 1α,25(OH)$_2$-20-epi-3-epi-D$_3$, the C-3 epimer of 1α,25(OH)$_2$-20-epi-D$_3$, was unequivocally identified using the techniques of UV absorption spectrophotometry, GC/MS analysis and co-elution with synthetic standard on both straight and reverse phase HPLC systems. As described in results section it was not possible to identify definitely the structures of metabolites Y1 and Y2 because of limited amounts of these metabolites available to us. Recently, we incubated UMR 106 cells with a different 20-epi vitamin D analog namely 1α,25(OH)$_2$-16-ene-20-epi-D$_3$ and found that this vitamin D analog is also metabolized into less polar metabolites. With the availability of milligram quantities of 1α,25(OH)$_2$-16-ene-20-epi-D$_3$ and its C-3 epimer, we were able to generate sufficient quantities of the less polar metabolites for ^{1}H-NMR analysis. The preliminary results suggested that the less polar metabolites are formed as a result of esterification of 1α-hydroxy group of the two 16-ene-20-epi vitamin D analogs with fatty acids [Reddy et al., unpublished observations]. Presently, we are in the process of identifying the chemical structures of the fatty acids. From these preliminary results, we assume that the less polar metabolites Y1 and Y2 are indeed C-1 fatty acid esters of 1α,25(OH)$_2$-20-epi-D$_3$ and its C-3 epimer, respectively.

Less polar metabolites, especially fatty acid esters of other steroid hormones have been identified in various tissues. This subject is recently reviewed [Hochberg, 1998]. At present we do not have enough information about the enzyme(s) responsible for the production of these LPMs. However, we noted that like the C-3 epimerization pathway, which is target tissue specific [Reddy et al., 1994, 1997, 2001; Bischof et al., 1998; Brown et al., 1999b; Siu-Caldera et al., 1999b; Sunita Rao et al., 2001], the new pathway is also tissue specific, as the formation of LPMs was only observed in rat osteosarcoma cells but not in the rat kidney [Siu-Caldera et al., 1999a]. Furthermore, like the C-3 epimerization pathway [Siu-Caldera et al., 1999b], the new pathway is also expressed in some tissues like, ROS 17/2.8 cells in which the C-24 oxidation pathway is not expressed (Fig. 7).

In our present study, we have shown that the VDR-mediated transcriptional activity of 1α,25 $(OH)_2$-3-epi-D_3, the C-3 epimer of the natural hormone, is significantly reduced when compared to its parent, 1α,25$(OH)_2D_3$. 1α,25$(OH)_2$-3-epi-D_3 was found to exhibit only 25% of the VDR-mediated transcriptional activity of its parent. Unlike 1α,25$(OH)_2$-3-epi-D_3, 1α,25 $(OH)_2$-20-epi-3-epi-D_3 was found to exhibit similar potency in inducing VDR-mediated transcriptional activity as its parent, 1α,25 $(OH)_2$-20-epi-D_3. This finding suggests that the "3-epi" modification with the combination of "20-epi" modification does not significantly reduce the VDR-mediated transcriptional activity. Further, in the present study we also show that the two new metabolites, Y1 and Y2, when compared to their respective parent compounds, 1α,25$(OH)_2$-20-epi-D_3 and 1α,25$(OH)_2$-20-epi-3-epi-D_3, are less active in inducing VDR-mediated transcriptional activity. Out of the two metabolites, Y1 has higher biological activity and its potency is almost equal to 1α,25$(OH)_2D_3$. Thus, these results suggest that unlike the rat kidney in which 1α,25$(OH)_2$-20-epi-D_3 is metabolized into bioactive intermediary metabolites only via the C-24 oxidation pathway [Siu-Caldera et al., 1999a]; the rat osteosarcoma cells metabolize 1α,25$(OH)_2$-20-epi-D_3 into additional bioactive intermediary metabolites derived not only via the previously established C-3 epimerization pathway but also via the new pathway described in this study.

In summary, we report for the first time tissue specific metabolism of 1α,25$(OH)_2$-20-epi-D_3 into several bioactive metabolites. These bioactive intermediary metabolites derived not only via the previously established C-24 oxidation and C-3 epimerization pathways but also via a new pathway together contribute significantly to the enhanced expression of the final biological activities attributed to their parent, 1α,25 $(OH)_2$-20-epi-D_3. Furthermore, our results also suggest for the first time that the tissue specific metabolism and accumulation of the bioactive intermediary metabolites in significant amounts in only some tissues can result in obvious tissue specific differences in the potency of 1α,25$(OH)_2$-20-epi-D_3.

REFERENCES

Binderup L, Latini S, Binderup E, Bretting C, Calverley M, Hansen K. 1991. 20-epi-vitamin D_3 analogues: a novel class of potent regulators of cell growth and immune responses. Biochem Pharmacol 42:1569–1575.

Bischof MG, Siu-Caldera M-L, Weiskopf A, Vouros P, Cross HS, Peterlik M, Reddy GS. 1998. Differentiation-related pathways of 1α,25-dihydroxycholecalciferol metabolism in human colon adenocarcinoma-derived Caco-2 cells: production of 1α,25-dihydroxy-3epi-cholecalciferol. Exp Cell Res 241:194–201.

Bouillon R, Okamura WH, Norman AW. 1995. Structure-function relationships in the vitamin D endocrine system. Endocrine Rev 16:200–257.

Brown AJ, Dusso A, Slatopolsky E. 1999a. Vitamin D. Am J Physiol 277:F157–F175.

Brown AJ, Ritter C, Slatopolsky E, Muralidharan KR, Okamura WH, Reddy GS. 1999b. 1α,25-dihydroxy-3-epi-vitamin D_3 a natural metabolite of 1α,25-dihydroxyvitamin D_3, is a potent suppressor of parathyroid hormone secretion. J Cell Biochem 73:106–113.

Dilworth FJ, Calverley MJ, Makin HL, Jones G. 1994. Increased biological activity of 20-epi-1,25-dihydroxyvitamin D_3 is due to reduced catabolism and altered protein binding. Biochem Pharmacol 47:987–993.

ElsterE, Heber D, Koeffler HP. 1996. 20-epi-vitamin D_3 analogs: potent modulators of proliferation and differentiation of breast cancer cell lines in vitro. Adv Exp Med biol 399:53–70.

Elstner E, Lee YY, Hashiya M, Pakkala S, Binderup L, Norman AW, Okamura WH, Koeffler HP. 1994. 1α,25-dihydroxy-20-epi-vitamin D_3: an extraordinary potent inhibitor of leukemic cell growth in vitro. Blood 84:1960–1967.

Gniadecki R. 1997. Effects of 1α,25-dihydroxy-24-oxo-16-ene-vitamin D_3 and its 20-epi analogues (MC 1288, MC 1301, KH 1060), on clonal keratinocyte growth: evidence for differentiation of keratinocyte stem cells and analysis of the modulatory effects of cytokines. Br J Pharmacol 120:1119–1127.

Hochberg R. 1998. Biological esterification of steroids. Endocrine Rev 19:331–348.

Ishizuka S, Norman AW. 1987. Metabolic pathways from 1α,25-dihydroxyvitamin D_3 to 1α,25-dihydroxyvitamin D_3-26,23-lactone. J Biol Chem 262:7165–7170.

Lopata MA, Cleveland DW, Sollner-Webb B. 1984. High level transient expression of a chloramphenicol acetyl transferase gene by DEAE-dextran mediated DNA transfection coupled with a dimethyl sulfoxide or glycerol shock treatment. Nucleic Acids Res 12:5707–5717.

Makin G, Lohnes D, Byford V, Ray R, Jones G. 1989. Target cell metabolism of 1,25-dihydroxyvitamin D_3 to calcitroic acid. J Biochem 262:173–180.

Ozono K, Liao SA, Kerner SA, Scott RA, Pike JW. 1990. The vitamin D-responsive element in the human osteocalcin gene. Association with a nuclear proto-oncogene enhancer. J Biol Chem 265:21881–21888.

Reddy GS, Tserng K-Y. 1989. Calcitroic acid, end product of renal metabolism of 1,25- dihydroxyvitamin D_3 through C-24 oxidation pathway. Biochemistry 28:1763–1769.

Reddy GS, Jones G, Kooh SW, Fraser D. 1982. Inhibition of 25-hydroxyvitamin D_3-1-hydroxylase by chronic metabolic acidosis. Am J Physiol 243:E265–E271.

Reddy GS, Tserng K-Y, Thomas BR, Dayal R, Norman AW. 1987. Isolation and identification of 1,23-dihydroxy-24,25,26,27-tetranorvitamin D_3 a new metabolite of

1,25-dihydroxyvitamin D_3 produced in rat kidney. Biochemistry 26:324–331.

Reddy GS, Muralidharan KR, Okamura WH, Tserng KY, McLane JA. 1994. Metabolism of 1α,25-dihydroxyvitamin D_3 and one of its A-ring diastereomer 1α,25-dihydroxy-3-epivitamin D_3 in neonatal human keratinocytes. In: Norman AW, Bouillon R, Thomasset M, editors. Vitamin D a pluripotent steroid hormone: structural studies, molecular endocrinology and clinical applications. New York: Walter de Gruyter, pp 172–173.

Reddy GS, Siu-Caldera ML, Schuster I, Astecker N, Tserng KY, Muralidharan KR, Okamura WH, McLane JA, Uskokovic MR. 1997. Target tissue specific metabolism of 1α,25-dihydroxyvitamin D_3through A-ring modification. In: Norman AW, Bouillon R, Thomasset M, editors. Vitamin D, chemistry, biology, and clinical applications of the steroid hormone, Riverside Califonia, pp 139–146.

Reddy GS, Muralidharan MR, Okamura WH, Tserng K-Y, McLane JA. 2001. Metabolism of 1α,25-dihydroxyvitamin D_3 and its C-3 epimer, 1α,25-dihydroxy-3-epivitamin D_3 in neonatal human keratinocytes. Steroids 66:441–450.

Siu-Caldera M-L, Sekimoto H, Peleg S, Nguyen C, Kissmeyer A-M, Binderup L, Weiskopf A, Vouros P, Uskokovic MR, Reddy GS. 1999a. Enhanced biological activity of 1α,25-dihydroxy-20-epi-vitamin D_3, the C-20 epimer of 1α,25-dihydroxyvitamin D_3, is in part due to its metabolism into stable intermediary metabolites with significant biological activity. J Steroid Biochem Mol Biol 71:111–121.

Siu-Caldera M-L, Sekimoto H, Weiskopf A, Vouros P, Muralidharan KR, Okamura WH, Bishop J, Norman AW, Uskokovic MR, Schuster I, Reddy GS. 1999b. Production of 1α,25-dihydroxy-3-epi-vitamin D_3 in two rat osteosarcoma cell lines (UMR 106 and ROS 17/2.8): existence of the C-3 epimerization pathway in ROS 17/2.8 cells in which the C-24 oxidation pathway is not expressed. Bone 24:457–463.

Sunita Rao D, Campbell MJ, Koeffler HP, Ishizuka S, Uskokovic MR, Spagnuolo P, Reddy GS. 2001. Metabolism of 1α,25-dihydroxyvitamin D_3 in human promyelocytic leukemia (HL-60) cells: in vitro biological activities of the natural metabolites of 1α,25-dihydroxyvitamin D_3 produced in HL-60 cells. Steroids 66:423–432.